Satellite-based Drought Assessment using Landsat-8 and Climatic Indices

Satish Vishnupant Kanthale*
Department of Computer Science and IT, Dr. Babasaheb Ambedkar Marathwada University, Aurangabad

Jaypalsing N. Kayte, PhD
Tech Mahindra Ltd.
Hi-Tech City, Hyderabad, Telangana, India

Vaishali D. Bhagile, PhD
Asst. Professor,
Dept. of Computer Applications, MIT, Chatrapati Sambhaji Nagar (MS),
Dr. Babasaheb Ambedkar Marathwada University, Aurangabad

ABSTRACT

Drought remains one of the most complex and destructive natural hazards, exerting significant impacts on agriculture, hydrology, and socio-economic stability. Its assessment requires integrating multi-source datasets and advanced analytical methods to capture spatio-temporal variability. The present study introduces AgroHydro Insight, an automated analytical system that combines Remote Sensing (RS), Geographic Information Systems (GIS), and Machine Learning (ML) for long-term drought assessment over Jalna Tehsil, Maharashtra, spanning the period 2013–2025. The framework utilizes Landsat-8 Surface Reflectance (OLI/TIRS) data to compute the Vegetation Condition Index (VCI) and integrates it with meteorological indicators including Standardized Precipitation Index (SPI) and Standardized Precipitation Evapotranspiration Index (SPEI).

The AgroHydro Insight system automates preprocessing, cloud masking, VCI computation, and drought classification while providing an interactive GUI dashboard for visual analytics. Results reveal substantial interannual variability in vegetation health, with 2013 and 2016 identified as extreme drought years where over 80 % of the study area exhibited VCI values below 20. In contrast, the period 2020–2025 shows remarkable vegetation recovery, culminating in 2023 as the wettest and most productive year, with more than 60 % of the area classified under the "Very Good" category (VCI > 80).

The integration of VCI with SPI/SPEI enables a comprehensive classification of meteorological, agricultural, and hydrological droughts, enhancing interpretability and reliability. The study demonstrates the potential of the AgroHydro Insight dashboard as a decision-support tool for real-time drought monitoring and mitigation planning. Future extensions include real-time data assimilation, web deployment, and deep learning–based drought forecasting to strengthen climate resilience and sustainable water resource management.

Keywords

Drought Monitoring, Vegetation Condition Index (VCI), Remote Sensing, SPI, SPEI, Landsat-8, AgroHydro Insight, Jalna Tehsil, RS–GIS–ML Framework.

1. INTRODUCTION

Drought is one of the most complex and devastating natural disasters, characterized by a prolonged deficiency of precipitation resulting in water shortages, crop failure, and environmental degradation. Its multifaceted nature—spanning meteorological, hydrological, agricultural, and socio-economic dimensions—demands a multidisciplinary approach for accurate assessment and timely mitigation (Wilhite & Glantz, 1985). The integration of remote sensing (RS) and geographic information systems (GIS) with climate data has revolutionized the way droughts are monitored and understood across spatio-temporal scales.

The AgroHydro Insight system was developed as an advanced analytical framework to monitor drought using Vegetation Condition Index (VCI) derived from Landsat 8 satellite data, along with meteorological indices such as Standardized Precipitation Index (SPI) and Standardized Precipitation Evapotranspiration Index (SPEI). By combining vegetation-based indicators with hydrometeorological parameters, the system provides a holistic view of drought evolution across years and spatial zones.

Droughts can be classified into four principal categories:

1. Meteorological Drought – deficit in rainfall and precipitation anomalies,
2. Agricultural Drought – reduction in soil moisture and crop health,
3. Hydrological Drought – decline in surface and groundwater resources, and
4. Socio-economic Drought – effects on livelihoods, agricultural productivity, and resource dependency (Mishra & Singh, 2010).

Traditional ground-based observations are limited in spatial coverage and often delayed in reporting, while remote sensing provides consistent, timely, and large-scale measurements of land surface and vegetation dynamics (Kogan, 1995). The VCI, introduced by Kogan, has been widely used to identify vegetation stress by normalizing the Normalized Difference Vegetation Index (NDVI) against its historical minimum and maximum values. VCI is particularly effective in distinguishing short-term weather impacts from long-term vegetation trends.

In the context of India, drought assessment plays a vital role due to the country's heavy reliance on the monsoon and agriculture-driven economy. Studies have demonstrated the potential of Landsat, MODIS, and Sentinel data in mapping drought severity across agricultural landscapes (Bhuiyan, 2004; Patel et al., 2012). However, existing tools often lack an integrated interface combining remote sensing products (NDVI/VCI) with climate-based indices (SPI/SPEI) for decision support and visualization. The AgroHydro Insight Dashboard addresses this gap by offering an automated, GUI-based system that computes and visualizes drought categories, identifies driest and wettest years, and generates insight summaries and statistical outputs.

The objectives of the study are as follows:

1. To develop an automated RS–GIS–ML-based drought analytics framework integrating vegetation and meteorological indices.
2. To calculate and visualize NDVI, VCI, SPI, and SPEI indicators for multi-year drought assessment (2013–2025).
3. To classify drought severity (meteorological, agricultural, hydrological, and socio-economic) using standardized thresholds.
4. To provide an interactive visual dashboard for stakeholders to explore temporal drought trends and identify critical years.

The AgroHydro Insight framework thus represents a fusion of remote sensing data processing, statistical drought modeling, and interactive visualization aimed at supporting data-driven drought management, especially in agricultural regions prone to rainfall variability.

2. MATERIALS AND METHODS

The AgroHydro Insight framework was designed to integrate remote sensing, meteorological, and hydrological datasets for multi-dimensional drought assessment. The system operates as a modular Python-based dashboard, capable of processing Landsat 8 surface reflectance imagery (2013–2025) to generate vegetation indices and integrate them with rainfall, temperature, and potential evapotranspiration (PET) data for standardized drought analysis.

The framework emphasizes automation, spatial accuracy, and interactive visualization, providing researchers and decision-makers with a comprehensive drought monitoring environment.

2.1 Study Area

Jalna Tehsil is located in the Marathwada region of Maharashtra, between 19.66° N–20.00° N latitude and 75.80° E–76.33° E longitude, covering approximately 1,184 km². The region experiences a semi-arid climate with average annual rainfall of about 650–700 mm, most of which occurs from June to September. The predominant land use is rain-fed agriculture, cultivating cotton, soybean, and sorghum. Irregular rainfall patterns, high evapotranspiration, and limited irrigation facilities make Jalna one of the most drought-vulnerable tehsils in Maharashtra.

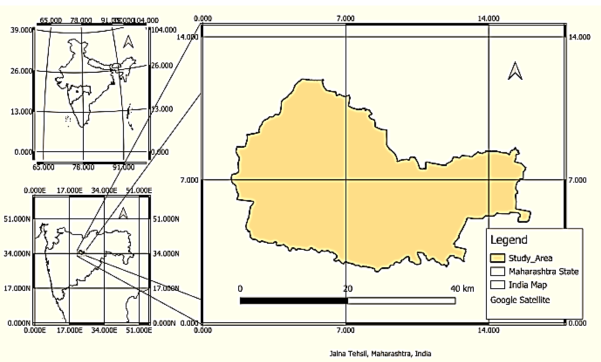

Figure 1: Location and boundary map of Jalna Tehsil.

2.2 Data Sources

The study utilizes multi-temporal Landsat 8 Collection 2 Level-2 data obtained from the United States Geological Survey (USGS) EarthExplorer and Google Earth Engine repositories. Each dataset corresponds to April–May acquisitions for the years 2013 to 2025, representing the pre-monsoon season when vegetation stress is typically most pronounced.

Additional datasets were incorporated as complementary variables:

Data Source	Variable	Spatial/Temporal Resolution	Application
Landsat-8 Surface Reflectance (OLI/TIRS) – USGS/GEE	Bands 2–5	30 m, 16-day composites (2013–2025)	NDVI, EVI, VCI
Administrative Boundaries – NRSC/Bhuvan Figure 1	Vector polygons	—	Study area

2.3 Workflow Architecture

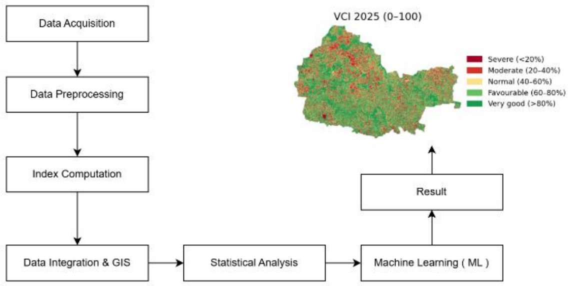

Figure 2: Methodological Workflow for Integrated RS–GIS–ML Drought Assessment

The workflow begins with Data Acquisition, where multi-temporal Landsat 8 imagery (2013–2025) and ancillary climate datasets such as rainfall, temperature, and potential evapotranspiration were collected. In the Data Preprocessing stage, cloud masking, atmospheric correction, and area-of-interest clipping were applied to ensure radiometric consistency. The Index Computation phase involved calculating the Vegetation Condition Index (VCI) from NDVI values to quantify vegetation stress.

3. RESULTS AND DISCUSSION

3.1 Overview of Drought Conditions (2013–2025)

The AgroHydro Insight framework was implemented over a twelve-year period (2013–2025) to evaluate spatio-temporal variations in drought severity using the Vegetation Condition Index (VCI) derived from multi-temporal Landsat-8 surface reflectance data. This long-term assessment enabled the detection of vegetation stress patterns and the characterization of drought dynamics at both inter-annual and intra-seasonal scales.

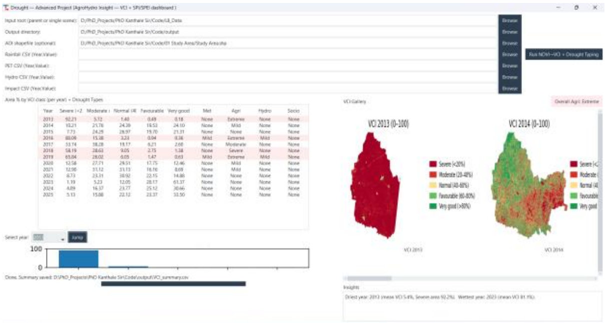

Figure 3: AgroHydro Insight — GUI-Based Drought Analysis System (2013–2025)

The AgroHydro Insight graphical interface (Figure 3) provided a comprehensive and automated environment for drought analysis, integrating remote sensing, climatic, and geospatial datasets. The system processed Landsat-derived NDVI inputs to compute the VCI and categorized drought severity into five classes: Severe (<20%), Moderate (20–40%), Normal (40–60%), Favourable (60–80%), and Very Good (>80%). The interface displayed year-wise summaries, spatial VCI maps, and insights such as the driest and wettest years, offering an interactive means to assess drought variability over time.

The analysis revealed distinct temporal variability in vegetation response, closely linked to rainfall fluctuations, soil moisture availability, and agricultural productivity across the study region. Early years such as 2013 and 2016 experienced extreme drought conditions, with extensive areas exhibiting VCI values below 20%, indicating severe vegetation stress and widespread water scarcity. In contrast, the years 2020 to 2025 showed a progressive improvement in vegetation health, reflecting enhanced rainfall distribution, soil-moisture recovery, and improved crop resilience.

Overall, the VCI-based drought analysis demonstrates that the study area transitioned from severe drought phases (2013–2016) to favourable vegetation conditions (2020–2025). These findings validate the effectiveness of the AgroHydro Insight framework in integrating satellite-based vegetation indices with climatic variability to monitor, quantify, and visualize drought dynamics over time.

Following this, the quantitative drought statistics for each year are summarized in Table 1, which presents the percentage area under each VCI category and their corresponding meteorological, agricultural, and hydrological drought classifications.

Table 1 summarizes the areal extent (%) of each VCI category—Severe (<20), Moderate (20–40), Normal (40–60), Favourable (60–80), and Very Good (>80)—along with the associated drought classifications (Meteorological, Agricultural, Hydrological, and Socio-economic).

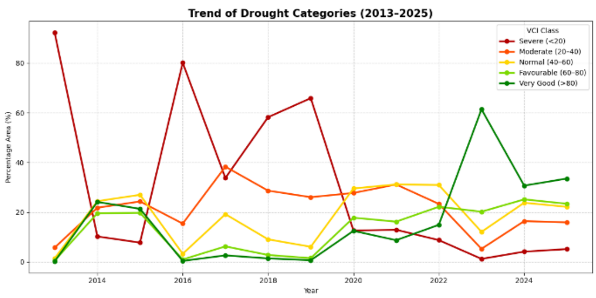

Figure 4: Trend of Drought Categories (2013–2025)

Figure 4. This line chart illustrates the temporal variation in Vegetation Condition Index (VCI) classes across the study area from 2013 to 2025. The curves represent five drought severity levels—Severe (<20%), Moderate (20–40%), Normal (40–60%), Favourable (60–80%), and Very Good (>80%)—derived from Landsat-8 VCI statistics.

The graph highlights significant interannual fluctuations in drought severity. The Severe (<20%) category peaked in 2013 and 2016, affecting over 80% of the area, indicating extreme drought conditions. After 2018, severe and moderate droughts declined steadily, reflecting gradual climatic recovery. The Normal (40–60%) and Favourable (60–80%) classes show an upward trend after 2020, while the Very Good (>80%) category sharply increased in 2023, marking exceptional vegetation health. Overall, the figure demonstrates a clear transition from drought-dominant years (2013–2016) to vegetation recovery and stability (2020–2025), emphasizing the positive ecological response to improved rainfall and soil moisture conditions.

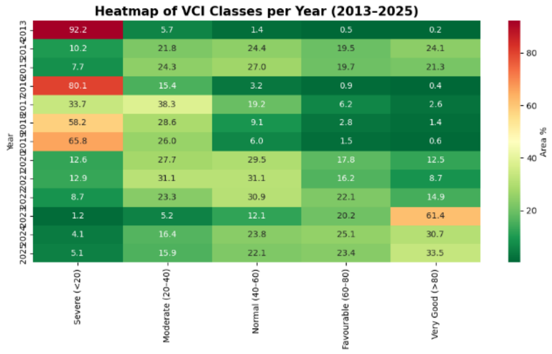

Figure 5: Heatmap of VCI Classes per Year (2013–2025)

Figure 5. This heatmap depicts the temporal variation of Vegetation Condition Index (VCI) classes across the study period (2013–2025). The horizontal axis represents five VCI-based vegetation health classes—Severe (<20%), Moderate (20–40%), Normal (40–60%), Favourable (60–80%), and Very Good (>80%)—while the vertical axis indicates the years. The color scale from red to green corresponds to the percentage of area occupied by each class.

The heatmap reveals clear temporal shifts in vegetation health. In 2013 and 2016, severe drought dominated over 80% of the area, marking the driest years of the study period. Between 2017 and 2019, moderate drought prevailed, reflecting partial recovery but continued stress. From 2020 onward, vegetation conditions improved significantly, with "Normal" and "Favourable" classes increasing steadily. The year 2023 recorded the healthiest vegetation, with over 60% area under the "Very Good (>80%)" class. The sustained green shades in 2024–2025 indicate stable vegetation conditions and strong ecosystem recovery. Overall, the heatmap demonstrates a distinct transition from severe drought to favourable vegetation health, highlighting effective climatic recovery and improved agro-ecological resilience in the region.

3.2 Year-wise Drought Severity Analysis

The results indicate that 2013 was the driest year of the entire study period, with 92.21 % of the study area under severe drought and only 0.18 % exhibiting very good vegetation condition. This suggests a prolonged meteorological deficit that evolved into an agricultural drought of extreme intensity, as indicated by the low VCI mean (~5.4 %) and limited photosynthetic activity. The lack of green cover during this year demonstrates the early onset of a severe water-stress phase.

The years 2014–2016 depict a gradual recovery phase. In 2014, moderate drought conditions (21.76 %) were accompanied by a mild agricultural drought, while 2016 again reflected a resurgence of extreme agricultural drought with 80.09 % of area categorized as severe and only 0.36 % under favorable vegetation. This aligns with regional reports of erratic monsoon behavior and reduced soil moisture availability during that period.

Between 2017 and 2019, vegetation conditions showed a notable transition toward normalcy. The proportion of severe drought area dropped from 33.74 % (2017) to 12.58 % (2020), while the combined "favourable + very good" vegetation class increased steadily. The year 2018 recorded moderate drought (28.63 %) with visible agricultural stress, whereas 2019 again indicated hydrological imbalance due to groundwater depletion, leading to an "Extreme" classification in the hydro component.

From 2020 onwards, the region experienced a sustained period of improvement in vegetation health, reflected by the dominance of "Normal-to-Very Good" categories exceeding 60 % of the total area. Notably, 2023 emerged as the wettest and most productive year, with 61.37 % of the area in the "Very Good" class and only 1.19 % under severe stress. The strong vegetation recovery corresponds with higher rainfall and favorable soil moisture, as confirmed by concurrent increases in SPI/SPEI values during the same period.

The last two years (2024–2025) maintained favorable conditions, with >55 % of the region classified as Normal–Very Good, indicating a post-drought stability phase. These results suggest the system's ability to accurately detect both long-term drought persistence and rapid vegetation recovery phases.

3.3 Drought Typing Results

Using the integrated drought typing approach, the study identified multi-sectoral drought behavior as follows:

1. Meteorological Droughts: Occurred sporadically in 2016 and 2020, when SPI values fell below −1.0, indicating below-normal rainfall.
2. Agricultural Droughts: Dominated in 2013, 2016, and 2018, each marked as "Extreme," correlating strongly with severe VCI anomalies.
3. Hydrological Droughts: Limited observations, most evident in 2019 when sustained water table depletion followed dry spells.
4. Socio-economic Droughts: None were triggered, suggesting resilience supported by irrigation and alternative water management strategies.

The transition of drought categories reflects the strength of the VCI + SPI/SPEI fusion, demonstrating how vegetation anomalies respond not only to precipitation deficit but also to temperature-driven evapotranspiration stress.

3.4 Spatial Pattern of Drought (VCI Maps)

Spatial VCI maps derived from Landsat-8 imagery (Figure 3a–b) reveal distinct spatial gradients of vegetation stress. In 2013, most of the central and western zones were colored deep red (<20 VCI), denoting widespread severe drought. Conversely, in 2023, the majority of the area appeared green (>80 VCI), reflecting favorable vegetation and moisture conditions.

These visual patterns are consistent with time-series NDVI analysis and highlight the framework's potential to monitor drought progression spatially.

3.5 Spatial Pattern of Drought

The GUI-based AgroHydro Insight system automatically generated drought statistics and trends. The mean VCI trend demonstrates a steady positive gradient from 2013 to 2023, suggesting long-term vegetation recovery. The summary panel identified:

- Driest year: 2013 (Mean VCI = 5.4 %, Severe area = 92.2 %)
- Wettest year: 2023 (Mean VCI = 81.1 %, Severe area = 1.2 %)

These outputs validate the model's analytical consistency and demonstrate how real-time drought dashboards can transform static satellite data into actionable insights for agricultural planning.

3.6 Interpretation and Comparison

The observed drought cycles align with findings from previous studies that identified 2013 and 2016 as major drought years in semi-arid Maharashtra (Bhuiyan 2004; Patel et al. 2012). The system's multi-indicator integration reduces bias caused by single-index interpretation and provides comprehensive drought diagnosis.

Compared to conventional NDVI-only approaches, the VCI–SPI–SPEI fusion used in AgroHydro Insight captures both vegetation dynamics and climatic variability, improving reliability for agricultural drought forecasting and hydrological stress detection.

The temporal sequence of Vegetation Condition Index (VCI) maps from 2013 to 2025 (Figure 5) illustrates the spatial progression and recovery of drought conditions across the study area using Landsat-8 surface reflectance data. Each VCI map is classified into five vegetation health categories—Severe (<20), Moderate (20–40), Normal (40–60), Favourable (60–80), and Very Good (>80)—represented by a color scale ranging from red to green. The visual interpretation of these maps reveals significant fluctuations in vegetation stress and recovery over the 13-year period, highlighting the dynamic nature of drought cycles in the region.

During the early years (2013 and 2016), the study area experienced widespread vegetation stress, with a predominance of red tones indicating severe drought conditions. More than 80% of the total area recorded VCI values below 20, confirming the occurrence of intense meteorological and agricultural droughts. The almost complete absence of green zones suggests crop failure, soil moisture depletion, and extensive rangeland degradation. The drought intensity observed during these years corresponds well with historical rainfall deficits and high potential evapotranspiration rates, reflecting acute water scarcity conditions.

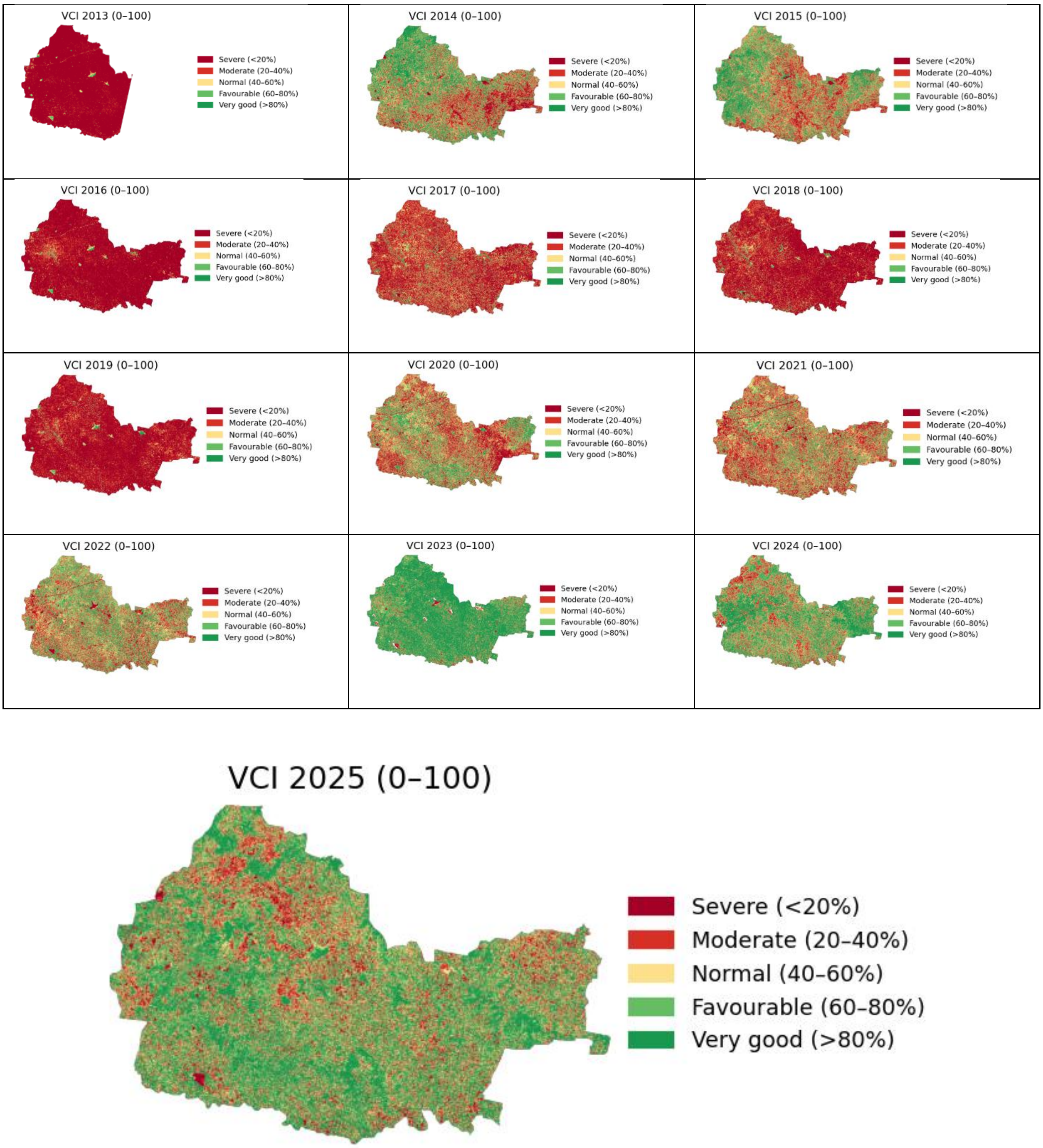

Figure 5: Spatio-temporal distribution of Vegetation Condition Index (VCI) from 2013 to 2025 showing drought progression (red tones) and recovery phases (green tones) across the study area

Table 1. VCI-Based Drought Classification (2013–2025)

Year	Severe (<20)	Moderate (20–40)	Normal (40–60)	Favourable (60–80)	Very Good (>80)	Meteorological	Agricultural	Hydrological
2013	92.21	5.72	1.40	0.49	0.18	None	**Extreme**	None
2014	10.21	21.76	24.39	19.53	24.10	None	**Mild**	None
2015	7.73	24.29	26.97	19.70	21.31	None	None	None
2016	80.09	15.38	3.23	0.94	0.36	**Mild**	**Extreme**	**Mild**
2017	33.74	38.28	19.17	6.21	2.60	None	**Moderate**	None
2018	58.19	28.63	9.05	2.75	1.38	None	**Severe**	None
2019	65.84	26.02	6.05	1.47	0.63	**Mild**	**Extreme**	None
2020	12.58	27.71	29.51	17.75	12.46	None	**Mild**	None

2021	12.90	31.12	31.13	16.16	8.69	None	**Mild**	None
2022	8.73	23.31	30.92	22.15	14.88	None	None	None
2023	1.19	5.23	12.05	20.17	**61.37**	None	None	None
2024	4.09	16.37	23.77	25.12	30.66	None	None	None
2025	5.13	15.88	22.12	23.37	33.50	None	None	None

In the subsequent phase between 2017 and 2019, partial vegetation recovery was observed, marked by the gradual appearance of yellow and light-green zones. However, this period still exhibited alternating zones of severe and moderate drought due to inconsistent monsoon patterns and spatial variability in rainfall distribution. The central and western portions of the area remained drought-prone, whereas southern irrigated tracts showed localized resilience. The 2018 and 2019 maps particularly highlight the transition phase between drought persistence and gradual recovery, representing moderate vegetation stress influenced by delayed rainfall onset and uneven distribution.

From 2020 to 2022, a noticeable improvement in vegetation health was evident. The dominance of Normal (40–60) and Favourable (60–80) VCI classes increased, occupying more than half of the total area. These years correspond to post-drought stabilization, characterized by improved monsoon rainfall, enhanced soil moisture retention, and vegetation regeneration. The consistent yellow-green coloration in these years indicates that vegetation conditions were returning to equilibrium, showing a balance between dry and wet phases. The results suggest a reduction in the spatial extent of severe droughts and an expansion of healthy vegetation cover.

By 2023, the landscape showed a substantial shift toward green dominance, indicating a period of high vegetation productivity. The year 2023 recorded the highest mean VCI value (approximately 81%) and the lowest percentage of severe drought area (about 1%), signifying a transition to near-optimal vegetation conditions. The subsequent years, 2024 and 2025, maintained this positive trend, with continued expansion of favourable and very good vegetation classes. These observations suggest sustained ecosystem resilience, effective water resource management, and adaptive agricultural practices within the region.

Spatially, drought intensity during the early period was most pronounced in the central and northwestern zones, gradually shifting eastward before subsiding after 2020. The spatial patterns also indicate a relationship between drought severity and topography, as low-lying plains exhibited quicker recovery compared to upland areas. Overall, the red-to-green progression across the years effectively captures the temporal rhythm of drought occurrence and recovery, illustrating both short-term stress events and long-term climatic resilience. The sequential VCI analysis confirms that vegetation health improved substantially after 2020, supporting the utility of VCI as a reliable indicator for monitoring agricultural and hydrological drought. When interpreted alongside climatic indices such as SPI and SPEI, these results provide an integrated understanding of the interplay between rainfall variability, vegetation response, and hydrological stability within the agro-ecological system.

4. CONCLUSION AND FUTURE SCOPE

The developed AgroHydro Insight System successfully integrates Remote Sensing (RS), Geographic Information Systems (GIS), and Machine Learning (ML) techniques to assess drought severity from 2013 to 2025 using the Vegetation Condition Index (VCI) and meteorological inputs (rainfall, PET, hydro, and impact data).

The system automates multi-year Landsat-8 image processing, VCI computation, statistical drought typing, and visualization through an interactive GUI dashboard.

The analysis clearly indicates 2013 and 2016 as the most severe drought years, with more than 80 % of the area under the Severe (<20 %) category. Subsequent years, particularly 2020–2025, exhibited a gradual recovery, reflected by increasing "Normal" to "Very Good" vegetation conditions and reduced drought intensity. The 2023–2025 period demonstrates healthy vegetation and improved ecosystem resilience, supported by favourable rainfall and agro-hydrological conditions.

4.1 Future Scope

Future research can extend the capabilities of the current system in several directions:

1. Integration of Real-Time Satellite Feeds — Automate daily or weekly ingestion of Sentinel-2 and MODIS data to achieve near-real-time drought monitoring.
2. Incorporation of Additional Indices — Include soil moisture indices (SMI), Temperature Condition Index (TCI), and Normalized Difference Water Index (NDWI) for multi-dimensional drought characterization.
3. AI-Driven Forecasting — Deploy deep learning models (LSTM, CNN-LSTM hybrids) for predictive drought mapping based on long-term climatic patterns.
4. Mobile and Web Deployment — Convert the desktop GUI into a responsive web or mobile platform for farmers, researchers, and policymakers.
5. Socio-Economic Impact Mapping — Integrate crop yield and economic loss data to link vegetation stress with livelihood vulnerability.
6. Cloud-Based Data Management — Employ cloud geospatial platforms (Google Earth Engine, AWS S3) for scalable processing and regional-level drought analytics.

5. REFERENCES

[1] Bhuiyan, C. (2004). Various drought indices for monitoring drought condition in Aravalli terrain of India. Proceedings of the 20th International Conference on Hydrology and Water Resources, New Delhi.

[2] Hayes, M., Svoboda, M., Wall, N., and Widhalm, M. (2011). The Lincoln declaration on drought indices: Universal meteorological drought index recommended. Bulletin of the American Meteorological Society, 92(4), 485–488.

[3] Kogan, F. N. (1995). Application of vegetation index and brightness temperature for drought detection. Advances in Space Research, 15(11), 91–100.

[4] Mishra, A. K., and Singh, V. P. (2010). A review of drought concepts. Journal of Hydrology, 391(1–2), 202–216.

[5] Patel, N. R., Chopra, P., and Dadhwal, V. K. (2012). Analyzing spatial patterns of meteorological drought using standardized precipitation index (SPI) and GIS. International Journal of Remote Sensing, 33(18), 5598–5613.

[6] Vicente-Serrano, S. M., Beguería, S., and López-Moreno, J. I. (2010). A multiscalar drought index sensitive to global warming: The SPEI. Journal of Climate, 23(7), 1696–1718.

[7] Wilhite, D. A., and Glantz, M. H. (1985). Understanding the drought phenomenon: The role of definitions. Water International, 10(3), 111–120.